Available online at www.sciencedirect.com
ScienceDirect
Trans. Nonferrous Met. Soc. China 20(2010) 2309−2313
Transactions of Nonferrous Metals Society of China
www.tnmsc.cn

Preparation and characterization of spinel $LiMn_2O_4$ nanorods as lithium-ion battery cathodes

CHEN Ze-hua(陈泽华) , HUANG Ke-long(黄可龙), LIU Su-qin(刘素琴), WANG Hai-yan(王海燕)
School of Chemistry and Chemical Engineering, Central South University, Changsha 410083, China

Received 11 December 2009; accepted 20 May 2010

Abstract: The hydrothermal synthesis of single-crystalline β-MnO_2 nanorods and their chemical conversion into single-crystalline $LiMn_2O_4$ nanorods by a simple solid-state reaction were reported. This method has the advantages of producing pure, single-phase and crystalline nanorods. The $LiMn_2O_4$ nanorods have an diameter of about 300 nm. The discharge capacity and cyclic performance of the batteries were investigated. The $LiMn_2O_4$ nanorods show better cyclic performance with a capacity retention ratio of 86.2% after 100 cycles. Battery cyclic studies reveal that the prepared $LiMn_2O_4$ nanorods have high capacity with a first discharge capacity of 128.7 mA·h/g.

Key words: spinel $LiMn_2O_4$ nanorods; β-MnO_2 nanorods; hydrothermal synthesis; solid-state reaction; electro-chemical properties

1 Introduction

Lithium-ion batteries are widely used in electronic devices, portable power tools, hybrid electric vehicles and many power supplies due to their high energy and power density. Spinel $LiMn_2O_4$ has been attractive in the field of lithium-ion batteries because of its high reduction potential, lower cost, and environmental impacts[1]. In general, as for the batteries application, it is believed that homogeneity, single-phase, uniform particle morphology with submicron size distribution, and large surface area are considered desired characters for achieving better electrode properties[2]. However, spinel $LiMn_2O_4$ synthesized by the conventional method has several disadvantages, such as inhomogeneity, large particle size, irregular morphology, broad particle size distribution, high synthesis temperature and repeated grinding[3]. It is believed that particle size seems to be a criterion which affects the electrochemical performance of cathode materials in Li-ion cells[4−5]. The small size of nano-metric particles can boost reactivity and shorten the diffusion paths which can increase the ability of electrodes to withstand high discharge rates over adequately long cycle life[6].

In this regard, development of nano-structured electrodes is attractive[7]. Nanomaterials are expected to exhibit improved functionality[8−9] due to their high surface area to volume ratio[10]. During recent years, researches were made to synthesize nano-crystalline $LiMn_2O_4$ particles. Wide ranges of wet chemical routes, such as sol-gel, co-precipitation and melt impregnation method, were investigated for the synthesis of nanocrystalline metal oxides with controlled physiochemical properties[2]. In this work, β-MnO_2 nanorods were synthesized through hydrothermal method. In order to obtain appropriate particle size, the $LiMn_2O_4$ nanorods were synthesized using the β-MnO_2 nanorods and $LiOH{\cdot}H_2O$ by a simple solid-state reaction. In addition, this synthesis method is considered to be inexpensive and simple. It is also the aim of the research to make comparison between normal powders and nano-powders in terms of their structure and electrochemical performance. The results indicate that as-prepared $LiMn_2O_4$ nanorods have better cycle performance and a higher charge storage capacity at higher rates.

2 Experimental

2.1 Experimental procedure

Analytical pure $MnSO_4{\cdot}H_2O$ and $NaClO_3$ and deionized water were used to prepare β-MnO_2 nanorods by hydrothermal reaction. 2.704 g $MnSO_4{\cdot}H_2O$ and

Foundation item: Project (2008AA031205) supported by the National High-tech Research and Development Program of China
Corresponding author: HUANG Ke-long; Tel: +86-731-88879850; E-mail:huangkelong@yahoo.com.cn
DOI: 10.1016/S1003-6326(10)60646-2

3.408 g $NaClO_3$ were dissolved in 60 mL deionized water to form homogeneous clear solution by magnetic stirring at room temperature. The mixed solution was transferred to a 100 mL Teflon-lined stainless steel autoclave and heated at 160 °C for 10 h in a preheated electric oven for the hydrothermal reaction. After the reaction, the final precipitated products were washed sequentially with deionized water and ethanol to remove the sulfate ions and other remnants by filtration. The obtained powder was sintered at 350 °C for 4 h in air.

The synthesis of $LiMn_2O_4$ nanorods was as follows: 0.06 g $LiOH·H_2O$ and 0.2434 g synthesized β-MnO_2 nanorods were dispersed into 5 mL pure ethanol to form a thick slurry, ground to form a fine mixture for several hours, and dried at room temperature[11]. The above process was repeated two or three times to produce well-mixed powder. The powder was calcined at 300 °C for 4 h and then calcined at 750 °C in air for 24 h.

2. 2 Electrochemical investigation

The electrodes for electrochemical studies were prepared by making a slurry of 85% (mass fraction) active material of $LiMn_2O_4$, 10% conducting carbon nano-tube, and 5% polytetrafluoroethylene as the solvent, which were coated on the pretreated steel reticulation. The coated cathode steel reticulation was pressed, cut into circular discs of 18 mm in diameter, and allowed to dry at 100 °C for 10 h under vacuum.

The button cells were assembled using 2016 stainless steel coin type containers in an argon-filled glove box. 1 mol/L solution of $LiPF_6$ in ethylene carbonate/ diethyl carbonate (V(EC)/V(DEC)=1:1) (Ferro Corporation) was used as the electrolyte. The charge-discharge cycles were preformed at different rates between 3.5−4.3 V at room temperature using LANDCT2001A. Electrochemical potential spectroscopy was also used to investigate the structural changes in the nanorods. X-ray diffraction (XRD) patterns were recorded on a Rigaku D/max-2500 diffractometer. SEM investigation of the powder was carried out on JSM−6360LV electron microscope.

3 Results and discussion

3.1 Morphology analysis of prepared β-MnO_2 and commercial MnO_2

Fig.1(a) shows the XRD pattern of the prepared β-MnO_2 and $LiMn_2O_4$ nanorods. Obviously, all the peaks in Fig.1(a) correspond to JCPDS data No.24—0735 having tetragonal symmetry with P42/mnm space group. In the meantime, the β-MnO_2 XRD diffraction shows that no additional impurity peaks have been detected. This implies that there are no other matters in the prepared β-MnO_2.

The morphology of β-MnO_2 particles was observed by SEM, as shown in Fig.2. It can be seen clearly that

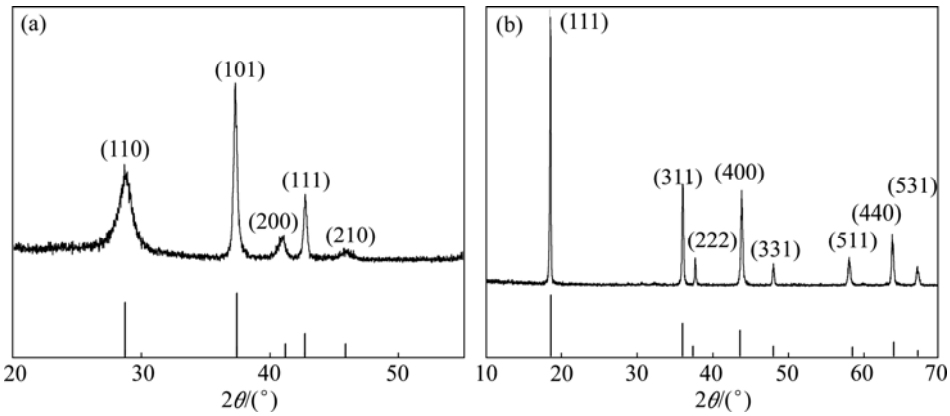

Fig.1 XRD patterns of prepared β-MnO_2 nanorods (a) and prepared $LiMn_2O_4$ nanorods (b)

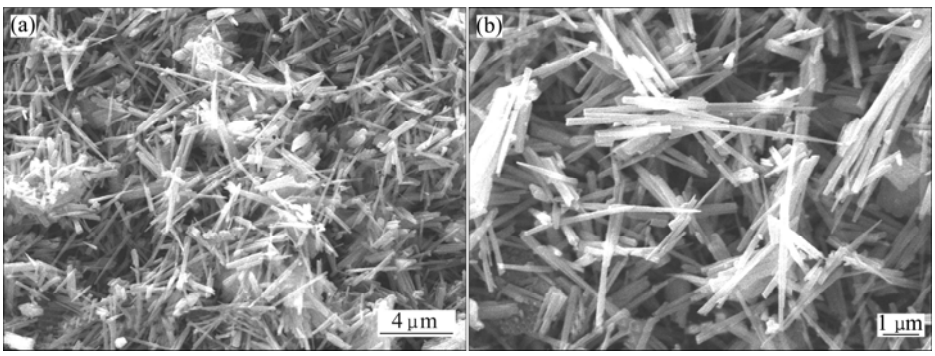

Fig.2 SEM images of β-MnO_2 as obtained by hydrothermal reaction

the β-MnO_2 power is composed of nanorods with the diameter of about 170 nm and the length of about 2.5 μm. They are well-proportioned and regular nanorods.

3.2 Morphology analysis of $LiMn_2O_4$ from different MnO_2

The XRD diffraction patterns of the $LiMn_2O_4$ nanorods (Fig.1(b)) show features of the spinel structure with Fd3m space group without peaks of the β-MnO_2 phase[11]. The reaction between β-MnO_2 and LiOH at 750 °C produced the pure $LiMn_2O_4$ nanorods phase. In the present work, we have synthesized dense, nano-crystalline $LiMn_2O_4$. The morphology of the nano $LiMn_2O_4$ crystals can be seen in Fig.3. We performed SEM analysis to confirm whether the nanorods morphology still remained after the high temperature solid-state reaction.

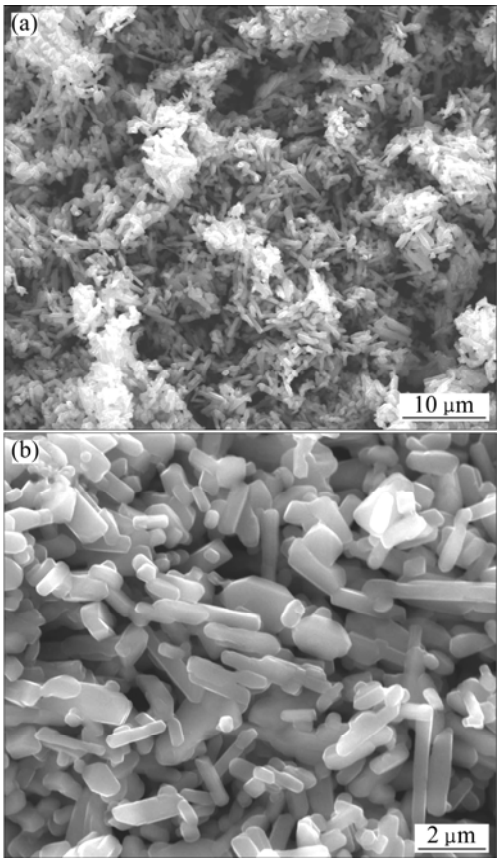

Fig.3 SEM images of $LiMn_2O_4$ prepared from β-MnO_2 nanorods

3.3 Electrochemical properties of batteries from different $LiMn_2O_4$

The discharge specific capacity of $LiMn_2O_4$ from the as-prepared $LiMn_2O_4$ nanorods and the generic $LiMn_2O_4$ from the commercial MnO_2 is displayed in Fig.4 as a function of cycle number. Fig.4 shows that the as-prepared nanorod material gives a discharge capacity of 128.7 mA·h/g in the first cycle. The generic $LiMn_2O_4$ exhibits an initial discharge capacity of 119.6 mA·h/g. Fig.4 shows that both the $LiMn_2O_4$ nanorods and the generic $LiMn_2O_4$ have two obvious horizontal discharge zones. The first horizontal zone is in the voltage range of 4.09–4.13 V and the other is in the range of 3.89–4.05 V. The shape is expected one for this spinel; two plateaus at ca. 4.0 and 3.8 V reflect the two-step process associated with the splitting of the original lithium positions of 8a in two sets of sites of 4a (0, 0, 0) and 4c (1/4, 1/4, 1/4), space group F23[6]. The two plateaus at about 4 V are due to the ordering of Li^+ in the tetrahedral sites or Mn ions in the octahedral (16d) sites, which corresponds to a cubic-to-cubic transition[6]. This shows that lithium ions embedded and disembodied in the $LiMn_2O_4$ powders in two stages. This result is also very similar to that reported in Ref.[12]. The most acceptable explanation is that particle size seems to be a criterion affecting the electrochemical performance of lithium ion battery cathodes in Li-ion cells[4−5]. The $LiMn_2O_4$ particle size is in the nanometer range with large specific surface area. Therefore, nano-materials exhibit improved functionality due to their high surface area to volume ratio[10].

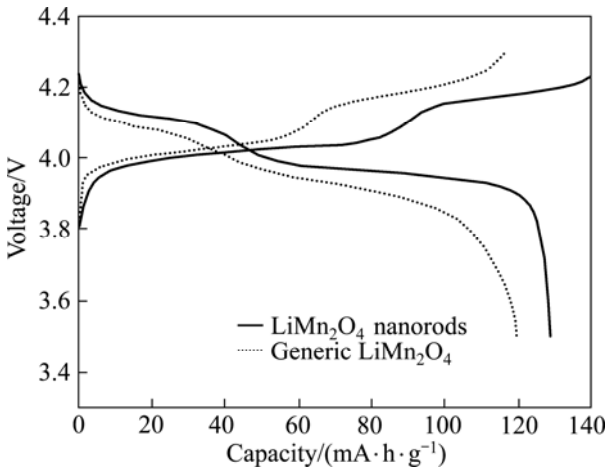

Fig.4 First charge-discharge curves of both samples at 0.1 *C* (1 *C*=148 mA/g)

In fact, the potential drop between the charge and the discharge process is measured between 0.1*C* and 1*C*. We have illustrated that the $LiMn_2O_4$ nanorods have a much higher discharge capacity than the generic $LiMn_2O_4$ at higher power rate. At the lowest current (from cycle 1 to 5), both the samples have specific capacity around 120 mA·h/g, but have a large difference in performance when the rate increases to 0.2*C* (from cycle 6 to 10). This specific capacity of the nanorods electrode remains almost 110 mA·h/g while that of the generic $LiMn_2O_4$ decreases to 70 mA·h/g. At 1*C*, nanorods electrode has higher specific charge capacity, probably because of the smaller size which leads to

improved charge transfer and smaller diffusion path lengths to active sites[13]. The reason for the high capacity is indicated in the X-ray diffraction results, which suggest that the $LiMn_2O_4$ nanorods obtained at 750 °C is a completely pure phase.

Fig.5(a) shows the discharge capacity as a function of cycle number for nanorods powder and the generic $LiMn_2O_4$. To evaluate the cycle ability of the nanorods electrode at a high rate, we have performed 100 cycles at 1*C*, as shown in Fig.5(b). It can be seen that the $LiMn_2O_4$ nanorods show very good capacity retention, and maintaining about 86.2% of its initial capacity 101.07 mA·h/g after 100 cycles; while, that of the generic $LiMn_2O_4$ maintains 55.06% of 89.16 mA·h/g after 100 cycles. The cycling capacity of the powder of the generic $LiMn_2O_4$ fade more quickly than that of the nanorods powder. Nanorods powder shows better cycling capacity. The $LiMn_2O_4$ nanorods powders possess higher charge-discharge cycling capacity than the generic $LiMn_2O_4$.

Fig.5(b) indicates that the $LiMn_2O_4$ nanorods display much smaller capacity loss of about 15 % than that of the generic $LiMn_2O_4$ about 45 % after charging 100 cycles. Because the nano-particles have large surface area-to-volume ratio and effective charge transfer,

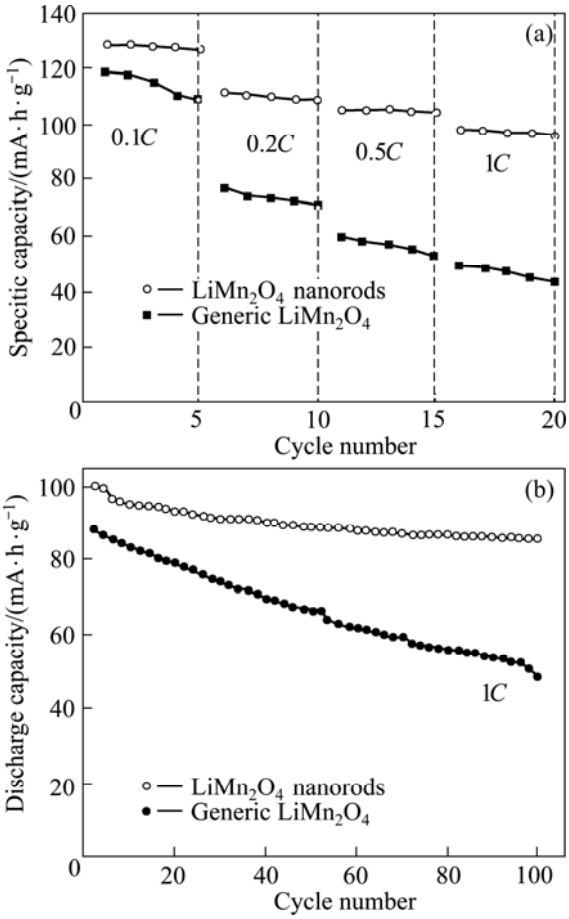

Fig.5 Discharge capacity as function of cycle number for both samples at various rates

correspondingly, it is illuminated that the capacity of the nano-crystalline materials is better the generic $LiMn_2O_4$[14]. Thus, nano-sized materials are beneficial to the diffusion of lithium-ion and noticeable improvement can be seen in our as-prepared $LiMn_2O_4$ nanorods compared with the generic $LiMn_2O_4$. The most reasonable explanation for this is that the surface area-to-volume ratio is larger, the ratio of atoms number on the surface to that in the interior is also larger than that of the generic $LiMn_2O_4$[15]. This indicates that a shorter path has to be traversed by Li^+ ions within the crystal domain[16]. This facilitates the transportation of ions through the cathode material into the electrolyte and onto the anode, which is required in a lithium rechargeable cell. The reason why the capacity of the generic $LiMn_2O_4$ fade quickly over cycles is also explained by the above discussion[17], which are believed to have increased the efficiency in the intercalation/de-intercalation process. In addition, faster Li^+ diffusion in the electrode materials would certainly improve the rate capabilities of Li-ion batteries. In the meantime, the effective charge transfer is also expected to be superior.

Hence, in this case, the well known enhanced lithium diffusion in the small particles of the prepared $LiMn_2O_4$ nanorods by this simple method has a significant effect. Therefore, the prepared $LiMn_2O_4$ nanorods can supply good capacity at high rates with good reversibility.

4 Conclusions

1) $LiMn_2O_4$ nanorods with cubic spinel structure have been obtained by scalable hydrothermal and solid-state reaction methods.

2) The X-ray diffraction patterns and the SEM image of the $LiMn_2O_4$ nanorods reveal the structure. The $LiMn_2O_4$ nanorods have an average diameter of 300 nm.

3) The $LiMn_2O_4$ nanorods show good capacity retention, maintaining about 86.2% of its initial capacity 101.07 mA·h/g after 100 cycles.

References

[1] VIVEKANANDHAN S, VENKATESWARLU M, SATYANARAYANA N, SURESH P, NAGARAJU D H, MUNICHANDRAIAH N. Effect of calcining temperature on the electrochemical performance of nanocrystalline $LiMn_2O_4$ powders prepared by polyethylene glycol (PEG-400) assisted Pechini process[J]. Materials Letters, 2006, 60: 3212–3216.

[2] HON Y M, LIN S P, FUNG K Z, HON M H. Synthesis and characterization of nano-$LiMn_2O_4$ powder by tartaricacid gel process[J]. European Ceramic Society, 2002, 22: 653–660.

[3] XIE Xing-hua, LI Xiao-jie, HONG Zheng-zhao, WU Bo, QU Yan-dong, HUANG Wen-yao. Growth and morphology of nanometer $LiMn_2O_4$ powder [J]. Powder Technology, 2006, 169:143–146.

[4] NAKAYAMA M, WATANABE K, KUTA H I, CHIMOTO Y U, WAKIHARA M. Grain size control of $LiMn_2O_4$ cathode material using microwave synthesis method [J]. Solid State Ionics, 2003, 164:35−42.

[5] BELIN T, GUIGUE-MILLOT N, CAILLOT T, AYMES D, NIEPCEIN J C. Fluence of grain size, oxygen stoichiometry, and synthesis conditions on the γ-Fe_2O_3 Vacancies ordering and lattice parameters [J]. Solid State Chem, 2002, 163:459−465.

[6] ARREBOLA J C, CABALLERO A, HERNÁN L. High performance hybrid lithium-ion batteries based on combinations of nanometric materials [J]. Nanotechnology, 2007, 18: 295705.

[7] DA S R, MAJUMDER S B, KATIYAR R S. Kinetic analysis of the Li^+ ion intercalation behavior of solution derived nano-crystalline lithium manganate thin films [J]. J Power Sources, 2005, 139: 261–268.

[8] KAMARULZAMAN N, YUSOFF R, KAMARUDIN N, SHAARI N H, ABDULAZIZ N A, BUSTAM M A. Investigation of cell parameter, microstructures and electrochemical behaviour of $LiMn_2O_4$ normal and nano powders [J]. J Power Sources, 2009, 188: 274–280.

[9] SCHOONMAN J. Nanoionics[J]. Solid State Ionics, 2003, 157: 319−326.

[10] JU S H, KANG Y C. Fine cathode particles prepared by solid-state reaction method using nano-sized precursor particles [J]. J Power Sources, 2007, 174: 1161−1166.

[11] YUNG D K, KIM M P, LEE H W, RICCARDO R. Spinel $LiMn_2O_4$ nanorods as lithium-ion battery cathodes [J]. Nano Lett, 2008, 8(11): 3948−3952.

[12] HON Y M, FUNG K Z, LIN S P, HON M H. Effects of metal ion sources on synthesis and electrochemical performance of spinel $LiMn_2O_4$ using tartaric acid gel process[J]. Solid State Chem, 2002, 163: 231−238.

[13] GAO Y, DAHN J R. $Li_x(Mn_{1-y}Co_y)O_2$ intercalation compounds as electrodes for lithium batteries[J]. Electrochem Soc, 1996, 143: 100−114.

[14] NIETO S, MAJUMDER S B, KATIYAR R S. Improvement of the cycleability of nano-crystalline lithium manganate cathodes by cation co-doping [J]. J Power Sources, 2004, 136: 88−98.

[15] YANG Yuan, XIE Chong, RUFFO R. Single nanorod devices for battery diagnostics: A case study on $LiMn_2O_4$ [J]. Nano Lett, 2009, 9(12): 4109−4114.

[16] OGATA A, SHIMIZU T, KOMABA S. Crystallization of $LiMn_2O_4$ observed with high temperature X-ray diffraction [J]. J Power Sources, 2007, 174: 756−760.

[17] WAN C, NULI Y, ZHUANG J, JIANG Z. Synthesis of spinel $LiMn_2O_4$ using direct solid state reaction [J]. Materials Letters, 2002, 56: 357−363.

(Edited by LI Xiang-qun)